



Improving electrochemical stability and electromechanical efficiency of ipmcs: tuning ionic liquid concentration

K. A. Tozzi^{1,2,3} · R. Gonçalves¹ · R. Barbosa¹ · M. C. Saccardo¹ · A. Zuquello⁴ · E. Sgreccia² · R. Narducci² · C. H. Scuracchio¹ · M. L. di Vona²

Received: 17 April 2022 / Accepted: 24 September 2022 / Published online: 12 October 2022
© The Author(s), under exclusive licence to Springer Nature B.V. 2022

Abstract

In the field of soft actuators, Ionomeric Polymer Metal Composites (IPMC)-like devices are a trend, exhibiting large displacement with low applied voltage. Its working mechanism is related to solvated electrolytes migration, thus the number of counterions exchanged with the polymeric membrane plays a key role in the device's performance. Although many kinds of inorganic and organic ions were used, there were few efforts to address a specific concentration value of electrolyte solutions. Ionic liquids (ILs) are used in IPMC to provide electrochemical stability; however, their mechanical performance is usually poor. In this study we aimed to determine a specific value of 1-butyl-3-methylimidazolium chloride ([BMIM]Cl) ionic liquid concentration between 0.1, 0.3, and 0.5 mol L⁻¹ that grants electrochemical stability at different relative humidities with best electromechanical efficiency. We synthesized [BMIM]Cl and characterized it through Nuclear Magnetic Resonance (NMR), Fourier Transform Infrared Spectroscopy (FTIR), and Cyclic Voltammetry (CV). The electrochemical behavior of Nafion[®]/Pt-based IPMC exchanged with IL was studied through Electrochemical Impedance Spectroscopy (EIS), CV, and Chronoamperometry (CA). Electromechanical properties were measured through blocking force and displacement. All the IPMC tests were carried out at three distinct controlled humidities (30%, 60%, and 90%). Herein, we tuned the IL concentration in 0.3 mol L⁻¹, delivering electrochemical stability with the best electromechanical yield regardless of the relative humidity. This result will be important when bringing electrolyte mixtures to further enhance the performance and efficiency of these devices.

✉ K. A. Tozzi
kiqtozzi@hotmail.com

¹ Department of Materials Engineering, Graduate Program in Materials Science and Engineering, Federal University of Sao Carlos (UFSCar), KM235, Rod. Washington Luís (SP-310), São Carlos, SP, Brazil

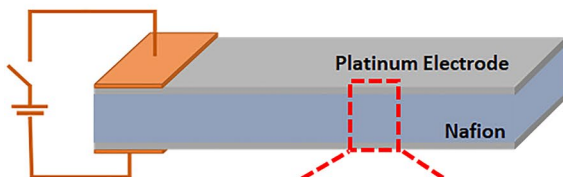
² Department of Industrial Engineering and International Laboratory "Ionomer Materials for Energy", University of Rome Tor Vergata, Via del Politecnico 1, 00133 Roma, Italy

³ Université Grenoble Alpes, Université Savoie Mont Blanc, CNRS, Grenoble INP, LEPMI, UMR5279, 38000 Grenoble, France

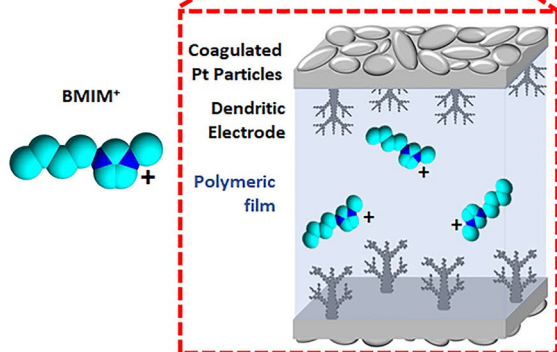
⁴ Community University of Chapecó Region, Polytechnic School, Chapecó, SC, Brazil

Graphical abstract

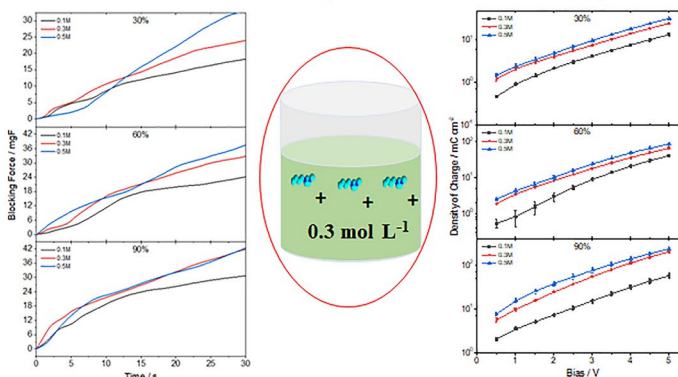
a Ionomeric Polymer-Metal Composites (IPMC)



b



c Electromechanical efficiency and electrochemical stability



Keywords Soft actuators · [BMIM]cl · Blocking force · EIS · Nafion®

1 Introduction

Ionic liquids (ILs) are very versatile materials since they have a broad range of applications, such as corrosion inhibitors [1], electrolytes in rechargeable batteries [2–5], additives for fuel cell application [6, 7], and also as green solvents when substitutes organic volatile compounds [8–10]. Properties such as low vapor pressure, hydrophilicity, and large electrochemical operation window are remarkable and play a key role in applying these substances in different research fields [11]. This usefulness arises from the huge number of possible combinations (10^{12}) between cations and anions to form an ionic liquid [12]. Then, complex systems where the properties above-mentioned are important to maintain stability throughout the lifetime or while working may consider ionic liquid's advantages.

Ionomeric polymer-metal composites (IPMCs) are electroactive devices with a metal/polymer/metal sandwich-based structure, capable of deforming in response to electrical stimuli and vice versa [13]. They have low density, flexibility, biocompatibility, and low drive voltage (< 5.0 V) [14]. Therefore, these piezoelectric devices are promising materials that can be applied as actuators [15–20], sensors [21–23], and also for energy harvesting applications [24]. This device's operation mechanism

consists of hydrated ions migration inside the polymer's ionomeric channels in response to an electric field generated after applying an electric potential to the metallic electrodes [19, 25]. For this reason, its electromechanical performance depends on several factors, such as electrical stimulus intensity [26, 27], membrane hydration level [28], and counterion type [29].

The most common types of counterions used are monovalent cations (H^+ , Li^+ , and Na^+) [29] divalent cations (Ca^{++} , Mg^{++} , and Ba^{++}) [30], and Ionic Liquids (IL) [31–33]. Okada et al., [34] found that the membranes' ionic conductivity depends on the ions' mobility, as well as the interaction of the ions with water molecules and charged species (SO_3^- groups). Motupally et al., [35] showed that alkali metals' ionic migration becomes greater when the cation ionic radius decreases. Consequently, IPMCs exchanged with monovalent counterions present an outstanding electromechanical response [29–31, 36]. On the other hand, monovalent and divalent cations have a high dependence on hydration processes, allowing the device to lose water by natural evaporation and electrolysis (when a voltage greater than 1.23 V is applied) [37]. Furthermore, the back relaxation phenomenon may occur due to water counter-diffusion [38] and water electrolysis in the vicinity of the electrodes [39]. For this reason, the use of IL in IPMCs to inhibit or attenuate electrolysis and back relaxation (that impairs mechanical performance) has grown dramatically [40–46].

Thus, devices based on IPMC (Ionomeric Polymer Metal Composite) are one example where handling ionic liquid may bring solutions against drawbacks such as water electrolysis (solvent loss) and back relaxation (that impairs mechanical performance), since ILs may grant electrochemical stability and also independence of environmental condition. Enhancing the IPMC performance is a way to achieve conditions to use it in real applications. Therefore, many different modifications ranging from the type of polymer membrane [47–49] to the electrode composition and assembly [40, 50–52] are being researched to meet the demands. Since the solvated counterions that neutralize the side chains of the most used membranes (e.g., Nafion® and SPEEK) are responsible for the different behaviors of the IPMC devices, one of the pathways to modulate the IPMC properties is exchanging different counterions inside the membrane.

One of the concerns about using ILs as electrolytes for IPMC is that the displacement and the blocking force were considerably lower when compared with other aqueous inorganic salts like lithium and sodium. Based on this assumption, one of the few works that attempted to fill the gap in modulating electrochemical and electromechanical behavior of these devices through the incorporation of mixtures of organic (e.g., ionic liquids) and inorganic counterions was the article of Safari et al. [53]. They tried to enhance the displacement of an IPMC device with lithium ions using different electrolyte concentrations. Regardless of this big effort, the authors did not conclude whether there is a minimum ionic liquid concentration that can be used to avoid the drawbacks previously discussed and how IL's presence may affect thermal, electrochemical, and electromechanical properties. Montazami et al. [54] tried to analyze the influence of ionic liquid concentration based on the soaking time of IPMC composed of Nafion®/poly(allylamine hydrochloride) and electrodes of Au nanoparticles, measuring also electrochemical and electromechanical properties. However, they did not consider that the amount of sulfated $-SO_3H$ side chains in Nafion® differed between samples as a function of soaking times, thus the properties would differ since what varied was not the concentration of the electrolyte itself.

Even in the most recently published papers, there is little information regarding the ionic liquid concentration or a reason to use a fixed value, rather than varying it [18, 55, 56]. As a consequence, it remains unclear how the molar concentration of ionic liquid influences the electrochemical and electromechanical properties. Furthermore, to use synergistic mixtures of organic and inorganic counterions, it would be interesting to find criteria or protocols that allow using all the advantages of each type of ionic species without side effects. For this reason, it is important to obtain parameters like an optimized molar concentration of one electrolyte type when bringing mixtures, boosting IPMC performance, since the concentration is related to

the quantity of ionic liquid inside the Nafion® ionomeric channels and the performance is associated with lower blocking force comparing with the usage of inorganic counterions. The low vapor pressure of ionic liquids may maintain the humidity level inside the membrane, preventing uncontrolled electrolysis.

Herein, we studied the effects of three different molar concentrations (0.1 mol L^{-1} , 0.3 mol L^{-1} , and 0.5 mol L^{-1}) of the ionic liquid 1-butyl-3-methyl-imidazolium chloride [BMIM]Cl on electrochemical, electromechanical, and thermal properties of an IPMC's composed of Nafion® 117 with platinum electrodes. As IPMC's capacitive-resistive behavior is of great importance, we carried out Electrochemical Impedance Spectroscopy (EIS), Chronoamperometry (CA), and Cyclic Voltammetry (CV) to verify the electrochemical properties. For these tests and the blocking force and tip displacement (electromechanical), we used a humidity control chamber to infer the minimum ionic liquid concentration that the IPMC should exchange to overcome the drawbacks of dry conditions and uncontrolled electrolysis. The humidity values followed the same scheme of IL concentration, i.e., 30%, 60%, and 90% (low, medium, high). Since we synthesized [BMIM]Cl by da Trindade method [57], we characterized the structure by NMR and FTIR, and also the electrochemical profile through CV before using it on IPMC.

The blocking force, displacement, and electrochemical measurements indicated that the IPMC exchanged with [BMIM]Cl at the molar concentration of 0.3 mol L^{-1} had the best balance between thermal, electromechanical, and electrochemical properties, hence we are addressing this value in our future works when attempting to use ionic mixtures to enhance IPMC performance.

2 Experimental

2.1 Materials

Nafion® 117 membranes were obtained from IonPower and were used after the following cleaning process: the membranes were boiled twice in H_2O_2 5% (v/v) (Sigma-Aldrich Corporation® analytical grade, used as received) solution for 30 min, then rinsed and boiled in 2 mol L^{-1} HCl for 30 min. Finally, they were rinsed and boiled in ultra-pure water for 30 min, and then the electroless plating was performed. Hydrochloric acid (HCl) (Sigma-Aldrich Corporation® analytical grade, used as received), tetraamineplatinum chloride ($Pt(NH_3)_4Cl_2$) – 98%, and sodium borohydride ($NaBH_4$) – 90% from Sigma-Aldrich Corporation® were used as precursors for the cleaning, ion diffusion, and reduction processes, respectively.

2.2 Ionic liquid synthesis

In a Schlenk flask, 80 mL of methylimidazolium (1 mol) was put to react with 125 mL of chlorobutane (1.2 mol) in 75 mL acetonitrile under argon reflux at 70 °C for 48 h. The resultant colorless liquid was precipitated in ethyl acetate under argon flux. The white precipitate, 1-butyl-3-methylimidazolium chloride, was dissolved in demineralized water in different concentrations.

2.3 Ionic liquid characterization

The ionic liquid structure was characterized through ^1H nuclear resonance spectra with a Bruker Avance 400 spectrometer apparatus (400.13 MHz) with D_2O as a solvent, where the chemical shifts are (ppm) referenced to tetramethylsilane (TMS).

ATR-FTIR spectrum was recorded in transmission mode from 4000 to 400 cm^{-1} with a Perkin-Elmer Spectrum 2 IR Spectrometer equipped with an ATR selenium crystal module. A background was run and the sample spectrum was normalized against the background spectra.

The solution voltammetric profiles at three different concentrations (0.1 mol L^{-1} , 0.3 mol L^{-1} , and 0.5 mol L^{-1}) were analyzed through Cyclic Voltammetry in a Potentiostat/Galvanostat Autolab PGSTAT 302 N employing a three-electrode cell using Pt (0.2 cm^2) as working electrode, from 0 to 5 V (same range used in IPMC devices) *versus* Ag/AgCl/KCl_(sat) (reference electrode) with a platinum wire as a counter electrode with a scan rate of 50 mV s^{-1} . The electrical conductivities were measured directly in IL solution using a conductivity meter from MS.

2.4 IPMC preparation

IPMC samples were prepared through electroless plating, as described in our previous works [17, 19, 27, 29]. The first step is the Nafion® surface cleaning with hydrochloric acid, diffusion of platinum cations (absorption), and reduction with sodium borohydride, forming a platinum thin layer of approximately 16 μm [27] that works as both electrodes

(cathode and anode). Reactions are depicted in the Table 1 below.

2.5 IPMC exchanging with [BMIM]Cl

Each IPMC sample was soaked in 25 mL of ionic liquid aqueous solutions with concentrations of 0.1, 0.3, and 0.5 mol L^{-1} for 24 h, therefore the samples were labeled regarding the [BMIM]Cl concentration. Solutions were prepared using ultrapure water (Milli-Q purification method).

2.6 Water uptake measurement

After exchanging with [BMIM]Cl, IPMC samples were dried at 120 °C in an air-ventilated oven, weighted (m_d), then rested at room temperature within 30%, 60%, and 90% relative humidity for 6 h, and weighed again (m_w). The % WU is calculated as:

$$WU = 100 * \left(\frac{m_w - m_d}{m_d} \right)$$

2.7 Electrochemical measurements

All the electrochemical measurements were performed in two electrodes mode. Using a Potentiostat/Galvanostat/EIS analyzer PalmSens4 cyclic voltammetry measurements were carried out at a rate of 100 mV s^{-1} in the bias range from -5 V to 5 V. Multi-step chronoamperometry was performed with bias from 0.5 to 5.0 V with a discharge between each 0.5 V of bias increment, where all the charge/discharge were held for 60 s. The charge densities were calculated by integrating the current *versus* time curves and normalizing them with the IPMC area. The electrical impedance data were done with an AC amplitude of 10 mV_{rms} and the frequency range from 0,01 MHz down to 10 mHz.

2.8 Electromechanical measurements

All electromechanical tests were carried out in a closed acrylic chamber with an atmosphere controlled by an

Table 1 Reactions in electroless plating of Pt in IPMC devices

Reaction	Description
$[\text{Pt}(\text{NH}_3)_4(\text{Cl})_2] + 2\text{NH}_4^+ + 2\text{OH}^- + 2\text{H}^+_{(\text{in Nafion})} \rightarrow [\text{Pt}(\text{NH}_3)_6]^{+2}_{(\text{in Nafion})} + 2\text{H}_2\text{O} + 2\text{Cl}^- + 2\text{H}^+$	Hydrolysis
$[\text{Pt}(\text{NH}_3)_6]^{+2}_{(\text{in Nafion})} \rightarrow \text{Pt}^{2+}_{(\text{in Nafion})} + 6\text{NH}_3$	Complex activation
$\text{Pt}^{+2}_{(\text{in Nafion})} + 2\text{NaBH}_4 \rightarrow \text{Pt}^0 + \text{H}_2 + \text{B}_2\text{H}_6 + 2\text{Na}^+_{(\text{in Nafion})}$	Redox reaction
$\text{B}_2\text{H}_6 + 6\text{H}_2\text{O} \rightarrow 2\text{B}(\text{OH})_3 + 6\text{H}_2$	Disproportionation
$[\text{Pt}(\text{NH}_3)_4(\text{Cl})_2] + 2\text{NH}_4^+ + 2\text{OH}^- + 2\text{H}^+_{(\text{in Nafion})} + 2\text{NaBH}_4 + 4\text{H}_2\text{O} \rightarrow \text{Pt}^0 + 7\text{H}_2 + 2\text{Na}^+_{(\text{in Nafion})} + 2\text{B}(\text{OH})_3 + 2\text{Cl}^- + 2\text{H}^+ + 6\text{NH}_3$	Global reaction

Arduino-based humidity and temperature control system. The samples were arranged in cantilever mode and actuated through an electrical control and monitoring system based on National Instruments (NI) modules. The tests were carried out as a function of potential and ambient humidity for the 30s. With the aid of a load cell, the blocking force was collected while the displaced sample was followed using a digital camera. Details of used equipment can be found in previous works.

3 Results and discussion

3.1 Ionic liquid characterization

Figure 1 shows the $^1\text{H-NMR}$ spectrum of [BMIM]Cl. The peaks from 0.80 to 4.05 ppm are assigned to the alkyl radicals, the peak at 3.80 ppm related to the methyl of methylimidazole used in the synthesis, while the other peaks to the butyl of chlorobutane. The other two peaks are related to the hydrogens that are shifted, as their positions on the molecular structure are near the quaternary nitrogen.

Regarding the purity of the self-obtained (synthesized) ionic liquid, the possible impurities could be the acetonitrile (2.06 ppm) and the methylimidazole (7.78 ppm) used as solvent and reactant, respectively [58]. As NMR is a highly sensitive technique and there is no trace of these two substances in the spectrum, the product has proper purity. ATR-FTIR spectrum in Fig. 1b was used with the same purpose as NMR Spectroscopy, e.g., to confirm the product of the synthesis. The high-intensity peak between 3330 and 3450 cm^{-1} arises from the presence of adsorbed water near the quaternary amine and chloride ionic interaction. The fewer intensity peaks at 2973–2870 cm^{-1} correspond to the stretchings and bendings of aliphatic groups (C–H). Finally, the stretching of double bonds, one between carbons and the other one between carbon and nitrogen (C=C and C=N), can be associated with the peaks at 1635 cm^{-1} and 1600 cm^{-1} , respectively, as the single bond between carbon and nitrogen is assigned with the peak at 840 cm^{-1} . These results made it possible to conclude that the ionic liquid was successfully synthesized. In the ionic liquid voltammograms (Fig. 1c), it is possible to see the electrochemical stability of the three

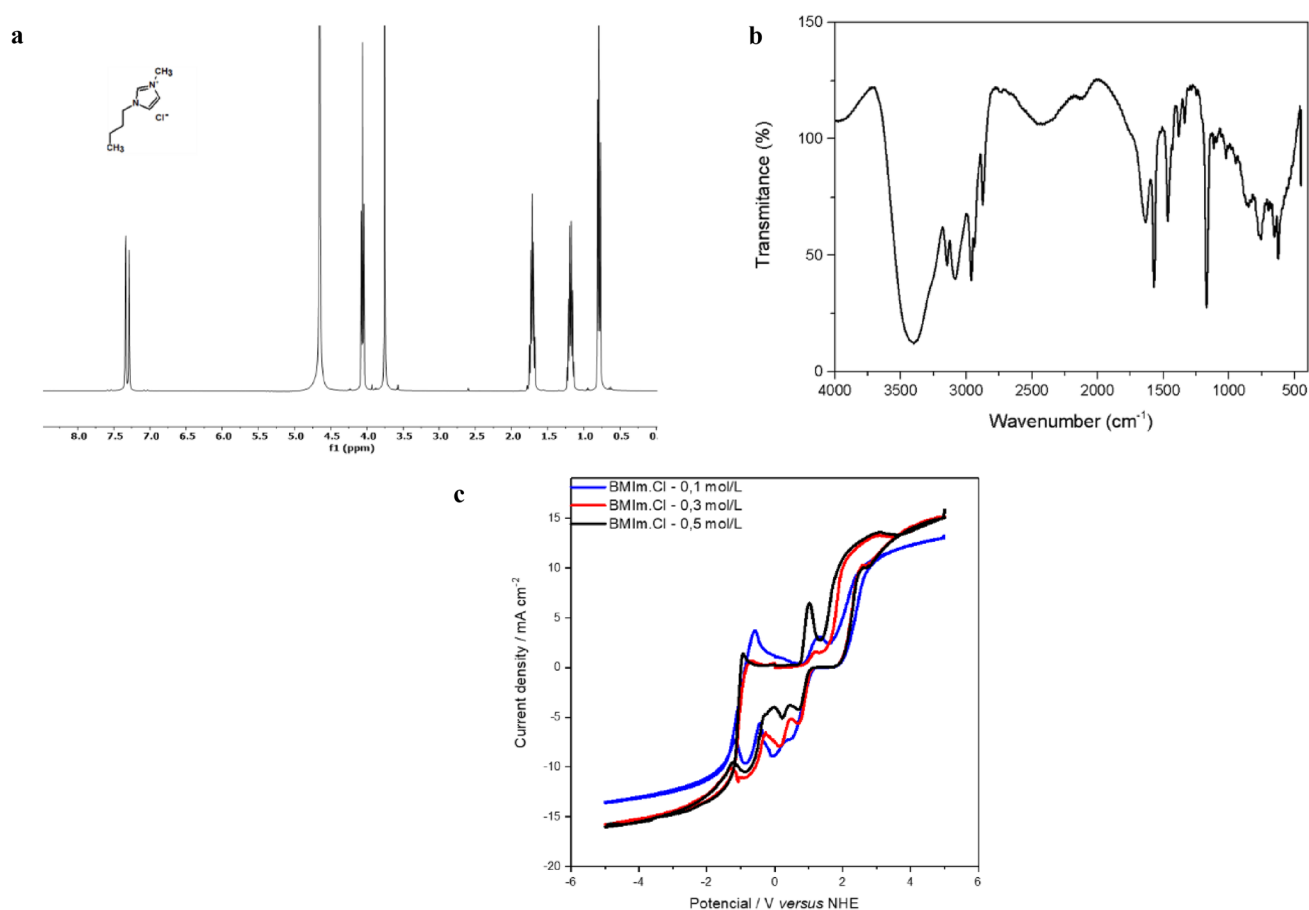


Fig. 1 [BMIM]Cl structure characterization: **a** $^1\text{H-NMR}$; **b** ATR-FTIR; **c** Cyclic Voltammetry

Table 2 Electrical characterization of [BMIM]Cl solutions

Concentration (mol L ⁻¹)	Electrolysis potential (through CV) (V)	Electrical conductivity (conductivity meter) (mS cm ⁻¹)
0.1	1.3	5.7
0.3	1.20	1.4
0.5	1.02	18.2

proposed concentrations, and Table 2 resumes the electrical properties of [BMIM]Cl solutions.

The water electrolysis normally occurs at 1.23 V. Still, as the electrical conductivity increases with higher electrolyte concentration and the [BMIM]⁺ provides stability to the solution, the Working Electrode (WE) value and the reversible cathodic reduction peak were shifted. The asymmetry seen in the results is due to the electrochemical stability of the cation and anion in ILs that decompose in higher voltages than 2.5 V [59], however, as can be seen in the next section, the voltammograms of IPMC with IL have reversible behavior, meaning that the ionic liquid remains inside the Nafion® structure without further decomposition in the applied range. Finally, the areas in the [BMIM]Cl voltammograms showed that the resistive behavior decays as the electrolyte concentration increases.

3.2 Electrochemical characterization

Water Uptake (WU) is directly related to hydrolytic stability and proton conductivity, being a standard measurement for ionomeric membranes. Figure 2 shows the WU of the IPMC devices exchanged with [BMIM]Cl in comparison with H⁺. As already exposed by Saccardo et al. [29], when an IPMC device is exchanged with counterions that have a small

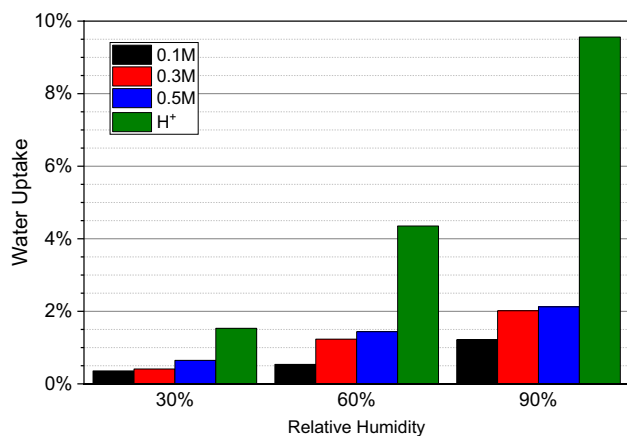


Fig. 2 Water Uptake (WU) of IPMC devices exchanged with 0.1, 0.3, and 0.5 mol L⁻¹ of [BMIM]Cl and H⁺ at different concentrations

radius (like H⁺), the device has a high water uptake. Here we confirm this observation and also address that between the three studied ionic liquid concentrations the WU is approximately the same, which means that the device experienced the same level of swelling, which is very important to maintain the electromechanical stability of the device. The small difference between the three proposed concentrations in the water uptake value is probably due to the reduction of the [BMIM]⁺ solvation shell in a smaller concentration (more water molecules around the side chain), since the pair H₃O⁺/SO₃⁻ is stable and would have also a thin layer of water molecules between the pair [BMIM]⁺/SO₃⁻ decreasing the water uptake.

Since the deformation in an IPMC device is related to the charge density that can be stored, evaluating the pseudo-capacitance, charge density, and other electrochemical properties is fundamental to understanding how to modulate the IPMC behavior. The voltammograms presented in Fig. 3 show that the concentration plays a key role in the capacitive-resistive behavior as the areas of 0.5 mol L⁻¹ samples are larger than the other ones at all humidity values. The profile seen in the graphs

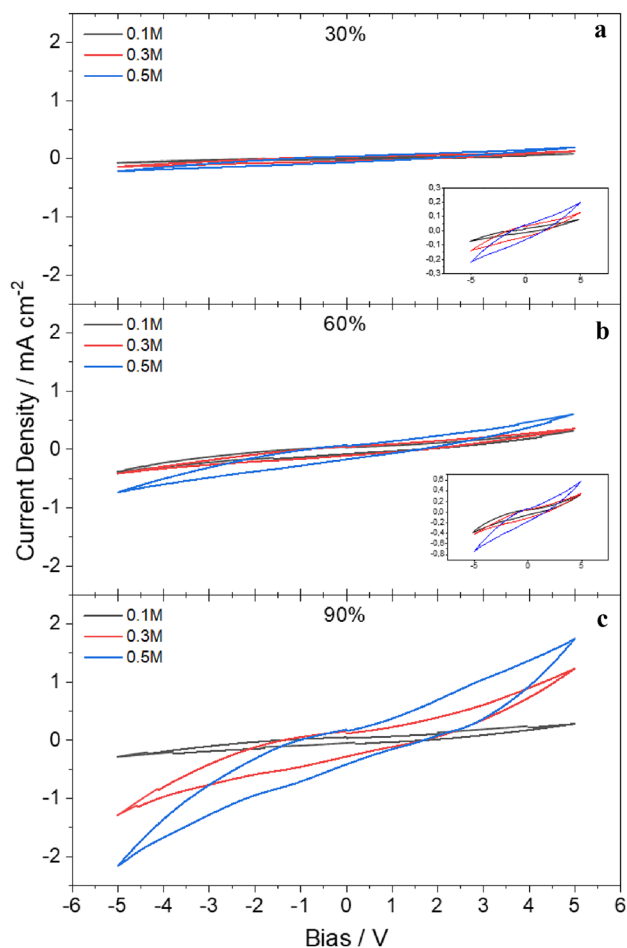


Fig. 3 Voltammograms at RH = **a** 30%, **b** 60%, and **c** 90%

is typical for IPMC exchanged with ionic liquids [27, 44, 45]. At all humidities, the double-layer capacitance increases with the [BMIM]Cl concentration indicating that more ionic species are adsorbed in the porous electrode surface, which is directly related to the vehicular diffusion mechanism [27], as there are more water molecules to solvate and diffuse charged species. It is also interesting that for a medium humidity (60%), the difference between the double-layer capacitance of 0.1 mol L⁻¹ and 0.3 mol L⁻¹ is small. Consequently, if an IPMC device is placed in this type of environment, the behavior of the device can be modulated by adding a small amount of [BMIM]Cl to give stability to the system while adding small inorganic cations (such as Li⁺) to increase its electromechanical properties [29]. Furthermore, the water electrolysis was indistinguishable even in the highest humidity. Regardless of a large number of water molecules available in the environment, the ionic liquid could prevent water loss inside the device even at the lowest concentration.

The specific capacitances C_p (F g⁻¹) of the devices were calculated through the areas of the voltammograms and are presented in Table 3. The C_p is calculated as:

$$C_p = \frac{A}{2km\Delta V}$$

Where: A voltammogram area, k scan rate, m electrolyte mass, ΔV bias window.

The results indicated that the device capacitance increased with raising electrolyte concentration and humidity.

The equivalent circuit used to fit the EIS data is shown in Fig. 4 [27], while the values of fitted elements are presented in Table 3. The EIS data seen in Fig. 5 and Table 4 were obtained to infer how the humidity and the concentration influence the processes occurring alongside the membrane and at the blocking electrode interface. The properties with ‘dev’ are related to the whole device, ‘char’ to the charging of the device, which depends on the size of the ionomeric channel, and ‘mch’ arises from the counterion migration from inner to outer channels.

Bode-plots have a good fitting at high frequencies, as the χ² < 10⁴ at low frequencies, the impedance follows a trend, i.e., the lowest concentration had higher impedance and the greatest concentration had lower impedance. This was expected since the device had a greater quantity of electrolytes that might have diffused, meaning that the charge separation was higher. On the other hand, at higher frequencies, 0.3 mol L⁻¹ and 0.5 mol L⁻¹ were quite similar, hence the ionic motion velocity of these two concentrations is approximately the same.

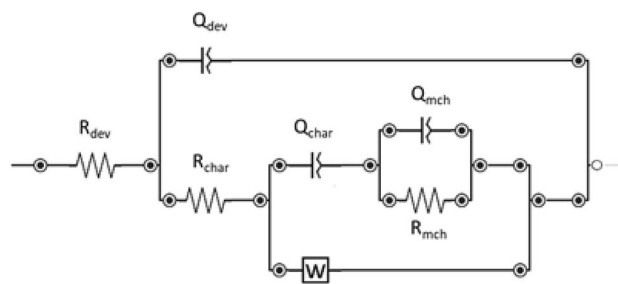


Fig. 4 Equivalent circuit

Regarding the device resistance (R_{dev}), the values are always lower for higher humidity conditions and concentration values, which was expected since this property is directly related to the membrane hydration degree and counterion [39]. However, for low humidity (30%), the increment in the ionic liquid concentration does not mean a decrease in the resistance device. In this case, it could be interesting to use the lowest concentrations of ionic liquid (0.1 mol L⁻¹) to provide electrochemical stability as could be seen in the voltammograms. On the other hand, for higher humidity (60% and 90%), the concentration decreased by one order of magnitude in R_{dev}.

The device capacitance (Q_{dev}) results corroborate the cyclic voltammetry profile and specific capacitance (C_p) calculated from the voltammograms, which means that the charge accumulation is faster for greater concentration and also higher when the humidity grows, as there are more water molecules to drag the counterions. However, the fitting for 90% humidity showed that the Q_{dev} is lower when compared with 30% and 60%. This is directly related to the swelling of the membrane since when RH=90%, there are many water molecules and counterion with a great size available inside the matrix that hinder charge separation. Hence, the pseudo-capacitance is lower when compared with other humidities, even for higher ionic liquid concentrations.

The R_{charge} is quite similar for low and medium humidity (30% and 60%), while for RH=90%, it becomes smaller. This was also expected since Nafion® has its ionic conductivity directly related to its hydration degree. Nevertheless, it is important to note that for RH=30%, this property was equal to RH=60%, indicating that even the lowest ionic liquid concentration was enough to counterbalance the absence of water molecules, which may enhance the usefulness of the device in dry conditions.

For the same IL concentration at different humidity, the Q_{char} increased more than one order of magnitude since the

Table 3 Devices specific capacitances

RH	RH 30%			RH 60%			RH 90%		
	0.1 M	0.3 M	0.5 M	0.1 M	0.3 M	0.5 M	0.1 M	0.3 M	0.5 M
C _p	2,26E-05	1,79E-05	1,52E-05	8,63E-05	3,60E-05	3,71E-05	9,40E-05	1,15E-04	1,17E-04

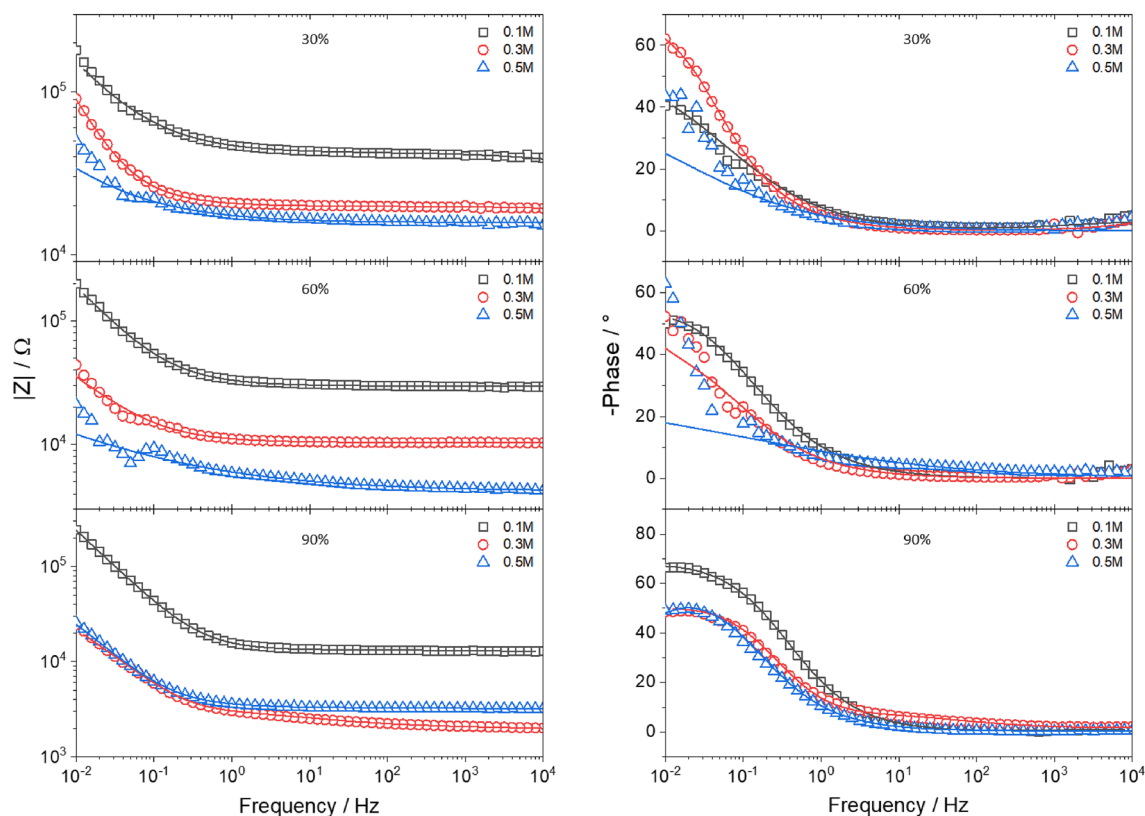


Fig. 5 Bode plots of IPMC exchanged with [BMIM]Cl at different humidities

Table 4 Impedance parameters from data fitting

RH	RH 30%			RH 60%			RH 90%		
	0.1 M	0.3 M	0.5 M	0.1 M	0.3 M	0.5 M	0.1 M	0.3 M	0.5 M
R_{dev}	3,44E+04	1,83E+04	1,57E+04	2,48E+04	9,62E+03	4,20E+03	3,01E+03	2,90E+03	7,65E+02
R_{char}	3,84E+05	5,47E+05	5,20E+05	1,52E+06	1,16E+05	3,84E+05	7,07E+03	3,43E+03	2,41E+03
R_{mch}	2,85E-08	1,00E+06	6,28E-02	2,27E-11	4,40E+05	2,35E-09	9,60E+02	1,37E+03	2,54E+02
Aw_1	7,93E+06	5,51E+06	1,82E+06	1,60E-11	1,67E+06	7,98E+06	1,88E+05	1,94E+05	3,53E+05
Q_{dev}	5,00E-05	1,29E-04	1,83E-04	4,83E-05	2,12E-04	2,85E-04	4,48E-10	1,29E-06	1,29E-05
n_{dev}	0,60	0,82	0,48	0,72	0,69	0,31	0,29	0,29	0,63E-15
Q_{char}	6,73E-08	2,60E-11	9,00E-07	1,53E-11	3,93E-04	2,05E-05	4,28E-05	1,80E-04	3,14E-04
n_{char}	0,72	0,925	1,00	1,79E-11	0,98	0,55	0,84	0,91	0,79
Q_{mch}	1,34E-04	1,03E-08	7,21E-05	4,36E-04	5,00E-04	4,42E-04	1,48E-14	1,16E-06	4,99E-04
n_{mch}	0,021	0,011	0,92	0,86	1,00	0,66	1,00	0,52	0,24
χ^2	1,89E-03	1,35E-04	8,13E-04	6,10E-04	3,77E-04	7,43E-04	9,57E-05	4,67E-04	2,38E-04

formation of the double-layer was influenced by the amount of water available to transport the mass of ionic liquid alongside the channels. Hence for the inner pseudo-capacitance, the humidity plays a key role and affects more than the counterion concentration. This is an interesting conclusion considering that the main reason for using ionic liquids in these devices is to maintain the membrane hydration degree. Finally, for the micro-channels RC properties, the model

used to discuss the membrane structure could not explain how these properties vary since the values have no congruency. Our next paper will debate the usage of a new model for fitting EIS data.

The device charge density calculated from the chronoamperometry test is presented in Fig. 6. The graphs are very clear about the similarity between 0.3 mol L⁻¹ and 0.5 mol L⁻¹ concentration, independently of the humidity

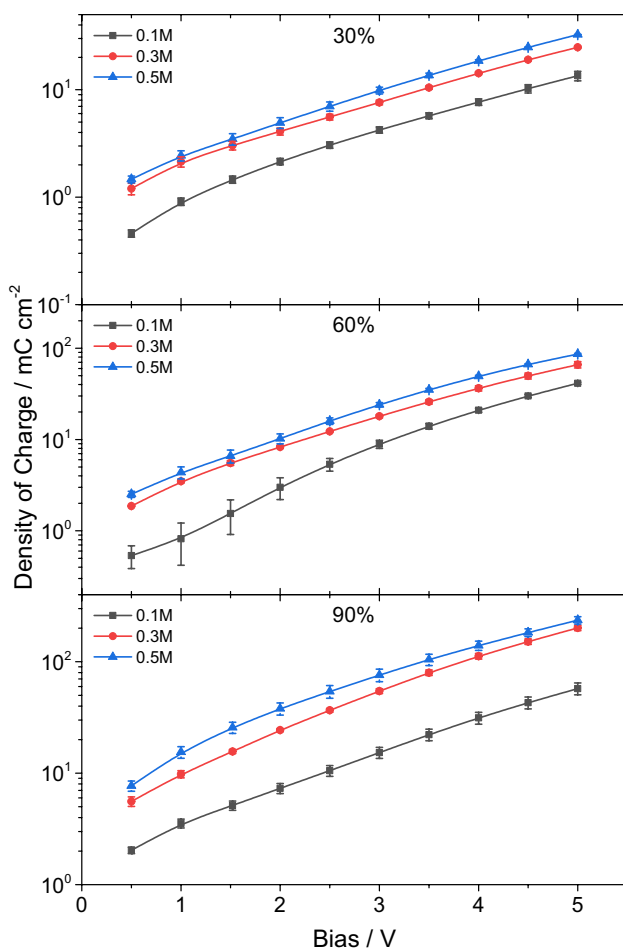


Fig. 6 Charge densities of IPMC exchanged with [BMIM]Cl at different humidities

level, as the values are quite similar. On the contrary, for 0.1 mol L^{-1} the humidity is crucial to grant a higher charge as it is possible to observe by comparing the graphs. The above-mentioned discussion of using 0.1 mol L^{-1} in dry conditions due to the similar value of R_{dev} is answered by these graphs. Although the resistance is the same, the charge density is crucial for electromechanical performance, and it is lower when using a low electrolyte concentration. However, the electrochemical properties studied herein suggest that the usage of 0.3 mol L^{-1} of IL is advantageous over 0.5 mol L^{-1} , as less IL is used and the inner channels of the membrane may be filled with inorganic ions in a mixture of electrolytes, providing better electromechanical properties [29] without losing electrochemical stability.

3.3 Electromechanical characterization

The IPMC electromechanical mechanism consists of the migration of solvated ionic charges throughout the ionomeric

channels driven by an electric potential. This ionic movement provokes an internal pressure gradient, leading to an anisotropic accumulation of mass (internal stresses) that causes the device's deformation [60]. Figure 7 resumes the mechanism of the IPMC actuator and also illustrates the methodology proposed for the usage of [BMIM]Cl.

Using the equipment already described in previous works [19, 27, 29], it was possible to characterize the electromechanical properties of the device with different concentrations of ionic liquids as a function of the relative humidity of the environment. At the same time, the current and electrical potential applied to the device were collected. All this information will be useful to calculate the electromechanical efficiency of the actuators. Figure 8a shows the displacement curves obtained by measuring each sample at different humidities operating with continuous 5 V of bias potential. Below 60% humidity, as there is an increase in the ionic liquid concentration, there is also an increase in the displacement value. An increase in the amount of BMIM molecules inside the ionomeric channels leads to an increase in the pressure gradient within the film, which leads to the bending of the device. However, at high humidity, 0.3 mol L^{-1} , and 0.5 mol L^{-1} , samples showed a very close performance. In addition, although the ionic liquid is not expected to be affected by the increase in humidity, the performance increase from 30 to 90% is noticeable.

On the other hand, in Fig. 8b it is possible to observe the blocking force exerted by the devices. Contrary to what is observed for displacement, the difference in performance between the concentrations is noticeable only at 30% of humidity. The response speed at 0.5 mol L^{-1} is very different from the others; this can be attributed to the low mobility of BMIM molecules added to the steric hindrance that one molecule exerts on the other, leading to a delay in the response. This is no longer observed at higher humidity since the polymer chains are more lubricated and have greater ionic mobility. The blocking force performance is very similar at high humidity, especially for 0.3 mol L^{-1} and 0.5 mol L^{-1} . Furthermore, the increase in blocking strength between 60% and 90% humidity is negligible, as expected for ionic liquids. However, comparing the two electromechanical parameters, one would expect that the performance of the blocking force corresponds to that of the displacement. Thus, the analysis of the shape of the curve, not reaching a plateau, suggests that the absorbed water molecules help to increase the mobility of the BMIM molecules, which causes the device to bend at a higher rate. However, these molecules do not actively participate in the ionic migration, thus, not increasing the force exerted by the device.

Although the devices operate at low potentials (below 5 V), when they work with smaller ions and a potential greater than 2 V is applied, there is a concern with their operating time as they are susceptible to electrolysis of water

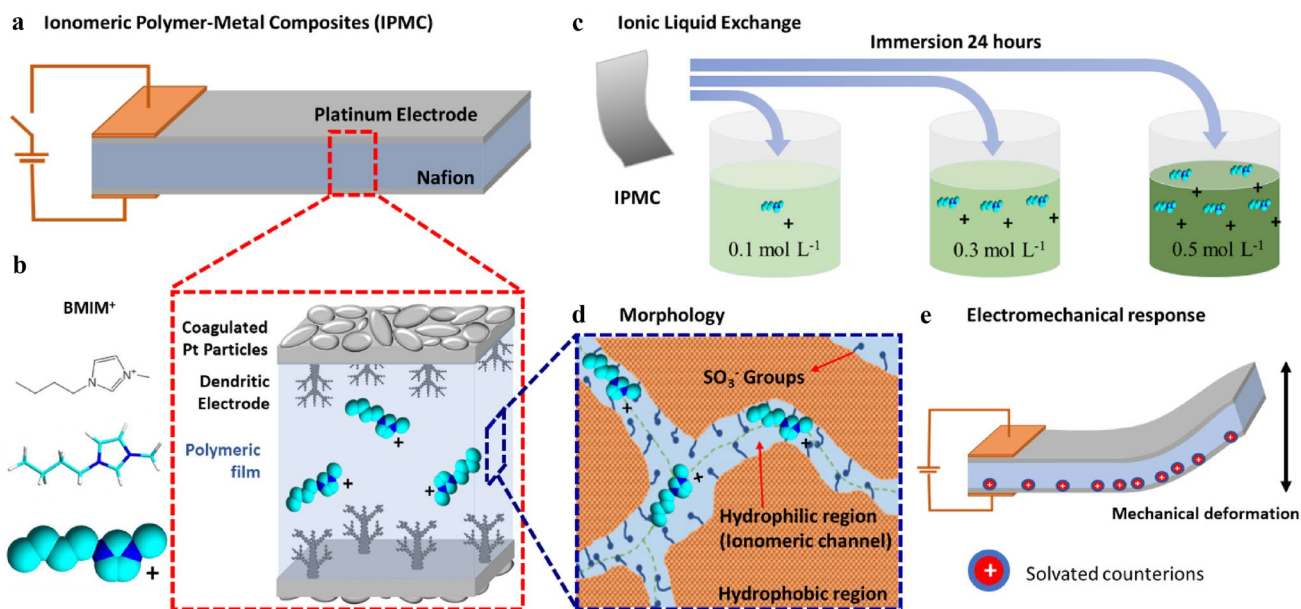


Fig. 7 **a** IPMC device composition; **b** schematic representation of [BMIM]Cl exchanged with IPMC device; **c** Work methodology; and **d** IPMC actuation mechanism

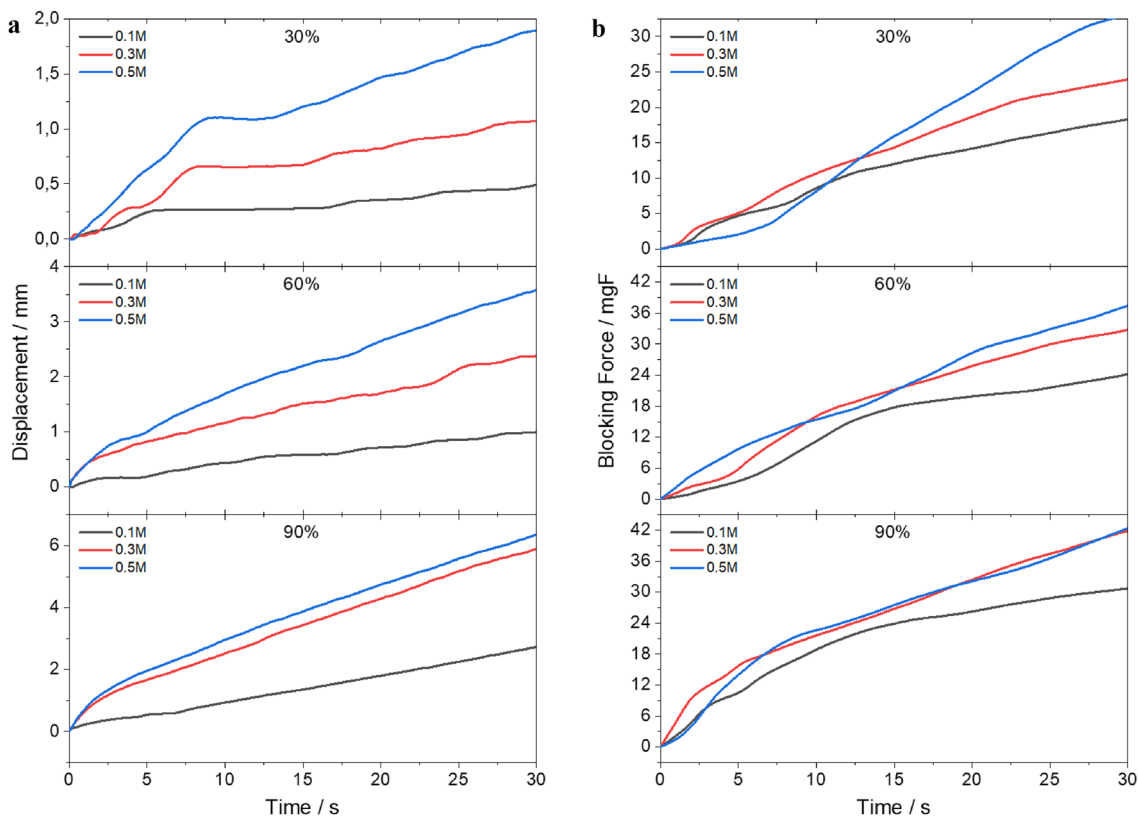


Fig. 8 **a** Displacement and **b** force curve as a function on application time of 5 V Bias

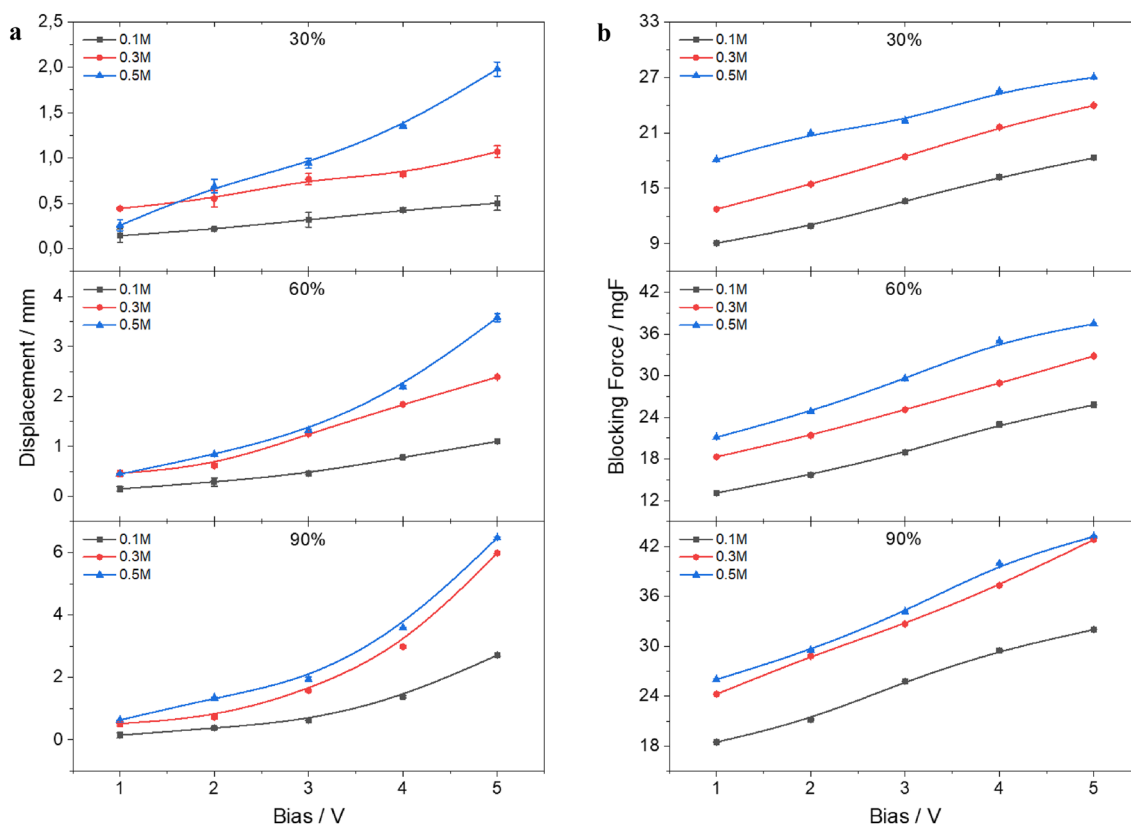


Fig. 9 **a** Displacement and **b** blocking force curves as a function of the applied Bias for different relative humidity and IL concentrations

accumulated in the ionic channels, causing the device to lose efficiency over time. One of the advantages of using ionic liquids is to minimize this drawback. Therefore, other operating potentials were tested. Figure 9 summarizes the maximum values of the electromechanical parameters as a function of the applied potential for each humidity and device tested. In support of the idea of low lubrication, the effect of low operating potential on the devices can be observed. A low potential corresponds to low energy supplied to trigger the device and promote ion migration, causing the device to move very little, almost imperceptibly. The concentration of 0.1 mol L^{-1} was the one with the smallest movements. On the other hand, at high humidity, it is possible to see a large effect exerted by the increase in the operating potential while exhibiting the same performance for concentrations of 0.3 mol L^{-1} and 0.5 mol L^{-1} .

Figure 9b shows the blocking force. For 30% and 60%, the response is linear for both the increase in potential and the increase in concentration, although the difference between them is very small. Regarding 90%, the response remains linear for the increase in potential, but the performance of 0.3 mol L^{-1} and 0.5 mol L^{-1} is the same. The presence of a linear response with the increase of the applied potential is expected because there is an increase in the electric field

gradient that makes the ions strongly attracted to the electrode by the electrostatic effect.

As previously mentioned, any potential and current variation during device operation can be recorded. With this information, other electrochemical parameters can be calculated for instance the charge used during the operation. It is then possible to obtain more “sophisticated” electromechanical parameters such as the operating efficiency involving the displacement value or blocking force normalized by the spent charge. Figure 10 shows these values as a function of the operating potential for all relative humidities and IL concentrations. In Fig. 10a, it is possible to observe the displacement efficiency values that indicate how much it is possible to obtain IPMC movement per charge unit. Interestingly, as there is an increase in humidity, there is a decrease in the efficiency of the device; that is, it uses more charge to perform the same amount of movement. The impact is greater in the sample with 0.1 mol L^{-1} that showed very low-efficiency values. Above 60%, it is also possible to observe for both 0.3 mol L^{-1} and 0.5 mol L^{-1} a drop-in efficiency with increasing potential up to 3 V and then a slight increase, inferring that efficiency would tend to increase even at higher potentials. With ionic liquids, this would be possible, as water electrolysis is no longer a concern, as concluded in previous works [27].

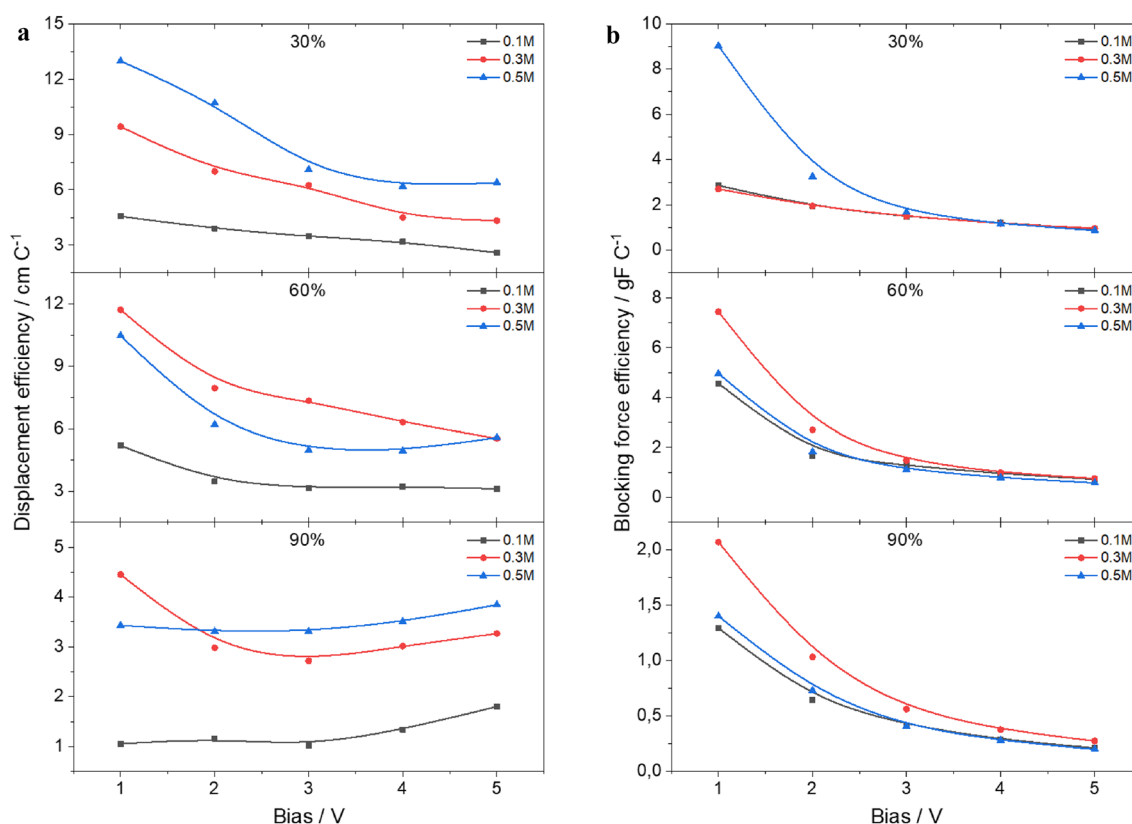


Fig. 10 **a** Displacement and **b** blocking force efficiency curves on applied Bias for different relative humidity and IL concentrations

On the other hand, in Fig. 10b, the blocking force efficiency is shown, demonstrating very different behaviors. The decrease in efficiency with the increase in potential is much more pronounced. At low humidity, the efficiency of the 0.5 mol L⁻¹ device is higher at low operating voltages; however, the concentration of 0.3 mol L⁻¹ had higher efficiencies at other humidities. Hence, at potentials above 3 V, the difference between the devices at any humidity tested is negligible. Therefore, in terms of economy, using a lower concentration of [BMIM]Cl, in this case, 0.3 mol L⁻¹, guarantees the same yield. At the same time, some drawbacks are minimized and in general, it can be said that this concentration has the best yield under the test conditions.

The rates of displacement and blocking force are also important to the device's efficiency since they are related to the time of deformation that it's also an important feature of the device application. Figure 11 presents these values with 5 V of Bias application. For the displacement rate, the results suggest that the concentrations of 0.3 mol L⁻¹ and 0.5 mol L⁻¹ are similar for medium and high humidities, having the same maximum displacement rate and both of them being higher than 0.1 mol L⁻¹ in any condition, while at low humidity 0.5 mol L⁻¹ concentration had a slightly better performance than the others, which corroborates with the Fig. 10a displacement efficiency graph. Regarding the

blocking force rate, the concentration of 0.3 mol L⁻¹ had higher peaks in all the conditions and reached to perform the maximum rate faster than the other concentrations in low and high humidities, being slower than 0.5 mol L⁻¹ just for the medium humidity, but still having a higher peak. The blocking force rate results reaffirm the behavior observed for the blocking force efficiency (Fig. 10b) and blocking force as a function of application time (Fig. 8b).

4 Conclusion

Ionic liquid [BMIM]Cl was successfully synthesized and its structure was confirmed through NMR, FTIR, and CV experiments. The IL was incorporated in the IPMC device based on Nafion and Pt electrodes in three different concentrations (0.1, 0.3, and 0.5 mol L⁻¹), and the electrochemical and electromechanical properties of the device were studied under controlled relative humidities.

The electrochemical study indicated that IPMC exchanging with 0.3 mol L⁻¹ allowed the same stability of 0.5 mol L⁻¹, and, beyond the economic advantage, there was also the possibility of filling the membrane inner channels with a higher number of inorganic counterions, which made it possible to modulate properties like electrical conductivity,

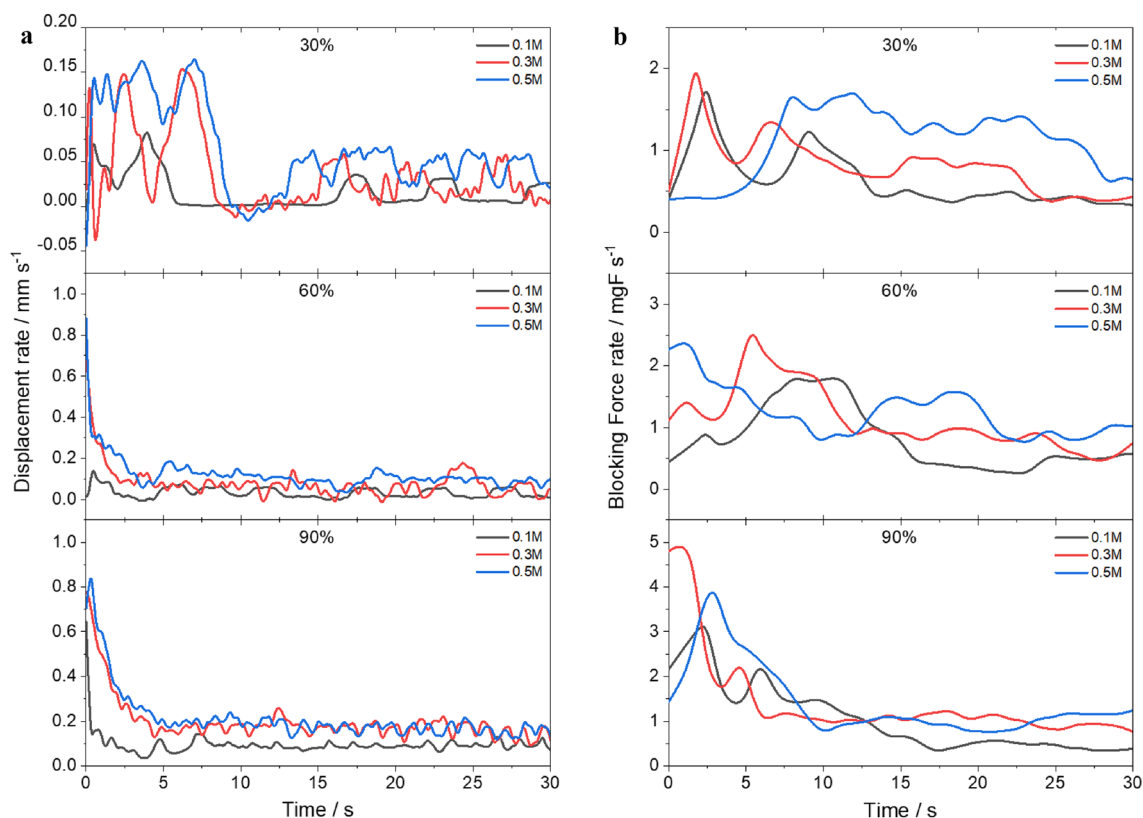


Fig. 11 **a** Displacement and **b** blocking force rate curves as a function of 5 V Bias for different relative humidity and IL concentrations

enhancing IPMC performance. Besides, even the smallest concentration of the ionic liquid could avoid the electrolysis phenomena, and it was possible to see that with a higher electrolyte concentration, the capacitive behavior was pronounced.

Mutually, the same concentration gave the best yield for electromechanical efficiency, corroborating what was observed before. We also highlighted the interesting effect that when the humidity increases, device efficiency decreases, i.e., IPMC uses more charge to perform the same displacement.

This paper attempted to fill the gap of a specific concentration value of ionic liquid exchanged with IPMC devices, and herein for [BMIM]Cl and Nafion®/Pt IPMC we addressed the concentration of 0.3 mol L^{-1} . We suggested, for future works, the usage not solely of this counterion but also of inorganic ones (like Li^+ and Na^+) to further enhance the performance and efficiency of these devices.

Acknowledgements This study was financed in part by the Coordenação de Aperfeiçoamento de Pessoal de Nível Superior - Brasil (CAPES) - Finance Code 001. We would like to thank the Coordenação de Aperfeiçoamento de Pessoal de Nível Superior - Brasil (CAPES) for the scholarships, processes: 88887.612843/2021-00, 88887.569936/2020-00, 23038.021524/2016-88. The authors would also like to thank the CNPq and Fundação de Amparo à Pesquisa do

Estado de São Paulo - Brasil (FAPESP) (process #2018/07001-6, #2018/10843-9, #2018/09761-8 and #2020/02696-6) funding agencies.

Declarations

Conflict of interest The authors have no competing interests to declare that are relevant to the content of this article.

References

1. Wu Y, Zhao W, Qiang Y, Chen Z, Wang L, Gao X (2020) Fang, π - π interaction between fluorinated reduced graphene oxide and acridinium ionic liquid: synthesis and anti-corrosion application. *Carbon N Y* 159:292–302. <https://doi.org/10.1016/j.carbon.2019.12.047>
2. Schmidt M, Heider U, Kuehner A, Oesten R, Jungnitz M, Ignat'ev N, Sartori P, (2001) Lithium fluoroalkylphosphates: a new class of conducting salts for electrolytes for high energy lithium-ion batteries. *J Power Sources* [https://doi.org/10.1016/S0378-7753\(01\)00640-1](https://doi.org/10.1016/S0378-7753(01)00640-1)
3. Giffin GA (2016) Ionic liquid-based electrolytes for “beyond lithium” battery technologies. *J Mater Chem A* 4:13378–13389. <https://doi.org/10.1039/c6ta05260f>
4. Macfarlane DR, Huang J, Forsyth M (1999) Lithium-doped plastic crystal electrolytes exhibiting fast ion conduction for secondary batteries. *Nature* 402:792–794. <https://doi.org/10.1038/45514>

5. Ito Y, Nohira T (2000) Non-conventional electrolytes for electrochemical applications. *Electrochim Acta* 45:2611–2622. [https://doi.org/10.1016/S0013-4686\(00\)00341-8](https://doi.org/10.1016/S0013-4686(00)00341-8)
6. Gang X (1993) Electrolyte additives for phosphoric acid fuel cells. *J Electrochem Soc* 140:896. <https://doi.org/10.1149/1.2056224>
7. Doyle M, Choi SK, Proulx G (2000) High-temperature proton conducting membranes based on perfluorinated ionomer membrane-ionic liquid composites. *J Electrochem Soc* 147:34. <https://doi.org/10.1149/1.1393153>
8. Quijano G, Couvert A, Amrane A, Darracq G, Couriol C, Le Cloirec P, Paquin L, Carrié D (2011) Potential of ionic liquids for VOC absorption and biodegradation in multiphase systems. *Chem Eng Sci* 66:2707–2712. <https://doi.org/10.1016/j.ces.2011.01.047>
9. Dupont J, Consorti CS, Spencer J, Room Temperature Molten Salts (2000) Neoteric “Green” solvents for chemical reactions and processes. *J Braz Chem Soc* 11:337–344. <https://doi.org/10.1590/S0103-5053200000400002>
10. Dupont J (2004) On the solid, liquid and solution structural organization of imidazolium ionic liquids. *J Braz Chem Soc* 15:341–350. <https://doi.org/10.1590/S0103-50532004000300002>
11. Consorti CS, De Souza RF, Dupont J, Suarez PAZ (2001) Líquidos iônicos contendo o cátion dialquilimidazólio: estrutura, propriedades físico-químicas e comportamento em solução. *Quim Nova* 24:830–837
12. Holbrey JD, Seddon KR, Liquids I (1999) *Clean Technol Environ Policy* 1:223–236. <https://doi.org/10.1007/s100980050036>
13. Bhandari B, Lee G-Y, Ahn S-H (2012) A review on IPMC material as actuators and sensors: fabrications, characteristics and applications. *Int J Precis Eng Manuf* 13:141–163. <https://doi.org/10.1007/s12541-012-0020-8>
14. Hao M, Wang Y, Zhu Z, He Q, Zhu D, Luo M (2019) A compact review of IPMC as soft actuator and sensor: current trends, challenges, and potential solutions from our recent work. *Front Robot AI* <https://doi.org/10.3389/frobt.2019.00129>
15. LI L, Guo X, Liu Y, Zhang D, Liao W-H (2022) Dynamic modeling of a fish tail actuated by IPMC actuator based on the absolute nodal coordinate formulation. *Smart Mater Struct* <https://doi.org/10.1088/1361-665X/ac8c0a>
16. Gupta A, Mukherjee S (2022) Actuation characteristics and experimental identification of IPMC actuator for underwater biomimetic robotic application. *Mater Today Proc* 62:7461–7466. <https://doi.org/10.1016/j.matpr.2022.03.388>
17. Zuquello AG, Saccardo MC, Gonçalves R, Tozzi KA, Barbosa R, Hirano LA, Scuracchio CH (2022) PI controller for IPMC actuators based on Nafion®/PT using machine vision for feedback response at different relative humidities. *Mater Res* <https://doi.org/10.1590/1980-5373-mr-2021-0518>
18. Wang HS, Cho J, Park HW, Jho JY, Park JH (2021) Ionic polymer–metal composite actuators driven by methylammonium formate for high-voltage and long-term operation. *J Ind Eng Chem* 96:194–201. <https://doi.org/10.1016/j.jiec.2021.01.021>
19. Saccardo MC, Zuquello AG, Gonçalves R, Tozzi KA, Barbosa R, Hirano LA, Scuracchio CH (2021) Electromechanical evaluation of ionomeric polymer-metal composites using video analysis. *Mater Res* <https://doi.org/10.1590/1980-5373-mr-2021-0317>
20. Ma S, Zhang Y, Liang Y, Ren L, Tian W, Ren L (2020) *Adv Funct Mater* 30:1–9. <https://doi.org/10.1002/adfm.201908508>. High-Performance Ionic-Polymer–Metal Composite: Toward Large-Deformation Fast-Response Artificial Muscles
21. Ostretsov KI, Orekhov YD, Khmelniitskiy IK, Aivazyan VM, Testov OA, Gareev KG, Testov DO, Karelin AM, Bagrets VS (2021) Heart Rate Monitor Based on IPMC Sensor. *Int Conf Electr Eng Photonics IEEE* <https://doi.org/10.1109/EEExPolytech53083.2021.9614697>
22. Das S, Ghosh S, Guin R, Das A, Das B, Saha S, Bhattacharya S, Bepari B, Bhaumik S (2022). IPMC as EMG Sensor to Diagn Human Arm Act https://doi.org/10.1007/978-981-16-7011-4_11
23. MohdIsa WH, Hunt A, HosseinNia SH (2019) Sensing and self-sensing actuation methods for ionic polymer-metal composite (IPMC): a review. *Sensors (Switzerland)* <https://doi.org/10.3390/s19183967>
24. Tiwari R, Kim KJ (2010) Disc-shaped ionic polymer metal composites for use in mechano-electrical applications. *Smart Mater Struct* <https://doi.org/10.1088/0964-1726/19/6/065016>
25. Ma S, Zhang Y, Liang Y, Ren L, Tian W, Ren L (2020) High-performance ionic-polymer–metal composite: toward large-deformation fast-response artificial muscles. *Adv Funct Mater* 30:1908508. <https://doi.org/10.1002/adfm.201908508>
26. Horiuchi T, Mihashi T, Fujikado T, Oshika T, Asaka K (2017) Voltage-controlled IPMC actuators for accommodating intraocular lens systems. *Smart Mater Struct* 26:045021. <https://doi.org/10.1088/1361-665X/aa61e8>
27. Gonçalves R, Tozzi KA, Saccardo MC, Zuquello AG, Scuracchio CH (2020) Nafion-based ionomeric polymer/metal composites operating in the air: theoretical and electrochemical analysis. *J Solid State Electrochem* <https://doi.org/10.1007/s10008-020-04520-6>
28. Bernat J, Kolota J (2018) Adaptive observer-based control for an IPMC actuator under varying humidity conditions. *Smart Mater Struct* 27:055004. <https://doi.org/10.1088/1361-665X/aab56e>
29. Saccardo MC, Zuquello AG, Tozzi KA, Gonçalves R, Hirano LA, Scuracchio CH (2020) Counter-ion and humidity effects on electromechanical properties of Nafion®/Pt composites. *Mater Chem Phys* <https://doi.org/10.1016/j.matchemphys.2020.122674>
30. Shahinpoor M, Kim KJ (2000) Effects of counter-ions on the performance of IPMCs, in: *Smart Structure Material 2000 Electroactive Polymer Actuators Devices, SPIE*, : p. 110 <https://doi.org/10.1117/12.387769>
31. Nemat-Nasser S, Wu Y (2003) Comparative experimental study of ionic polymer–metal composites with different backbone ionomers and in various cation forms. *J Appl Phys* 93:5255–5267. <https://doi.org/10.1063/1.1563300>
32. Correia DM, Barbosa JC, Costa CM, Reis PM, Esperança JMSS, De Zea Bermudez V, Lanceros-Méndez S (2019) Poly(vinylidene fluoride)-based soft actuators. *J Phys Chem C* 123:12744–12752. <https://doi.org/10.1021/acs.jpcc.9b00868>
33. Liu Y, Liu S, Lin J, Wang D, Jain V, Montazami R, Heflin JR, Li J, Madsen L (2010) Zhang QM (2010) transports of ionic liquids in ionic polymer conductor network composite actuators. *Electroact Polym Acta Dev* 7642:76421A. <https://doi.org/10.1117/12.847618>
34. Okada T, Xie G, Gorseth O, Kjelstrup S, Nakamura N, Arimura T (1998) Ion and water transport characteristics of Nafion membranes as electrolytes. *Electrochim Acta* 43:3741–3747. [https://doi.org/10.1016/S0013-4686\(98\)00132-7](https://doi.org/10.1016/S0013-4686(98)00132-7)
35. Motupally S, Becker AJ, Weidner JW (2000) Diffusion of water in Nafion 115 membranes. *J Electrochem Soc* 147:3171–3177. <https://doi.org/10.1149/1.1393879>
36. Onishi K, Sewa S, Asaka K, Fujiwara N, Oguro K (2001) The effects of counter ions on characterization and performance of a solid polymer electrolyte actuator. *Electrochim Acta* 46:1233–1241. [https://doi.org/10.1016/S0013-4686\(00\)00695-2](https://doi.org/10.1016/S0013-4686(00)00695-2)
37. Hwan Lee S, Cho E, Ryou J, Youn (2007) Rheological behavior of polypropylene/layered silicate nanocomposites prepared by melt compounding in shear and elongational flows. *J Appl Polym Sci* 103:3506–3515. <https://doi.org/10.1002/app.25204>
38. Shahinpoor M (2016) Fundamentals of ionic polymer metal composites (IPMCs), in: *RSC smart mater*. Royal Soc Chem <https://doi.org/10.1039/9781782622581-00001>
39. Leronni A, Bardella L (2021) Modeling actuation and sensing in ionic polymer metal composites by electrochemo-poromechanics. *J Mech Phys Solids* 148:104292. <https://doi.org/10.1016/j.jmps.2021.104292>

40. Duncan AJ, Sarles SA, Leo DJ, Long TE, Akle BJ, Bennett MD (2008) Optimization of active electrodes for novel ionomer-based ionic polymer transducers. *Electroact Polym Actuators Devices* 2008 6927:69271Q. <https://doi.org/10.1117/12.776575>
41. Green MD, Wang D, Hemp ST, Choi JH, Winey KI, Heflin JR, Long TE (2012) Synthesis of imidazolium ABA triblock copolymers for electromechanical transducers. *Polym (Guilfd)* 53:3677–3686. <https://doi.org/10.1016/j.polymer.2012.06.023>
42. Margareta E, Fahs GB, Inglefield DL, Jangu C, Wang D, Heflin JR, Moore RB, Long TE (2016) Imidazolium-containing ABA triblock copolymers as electroactive devices. *ACS Appl Mater Interfaces* 8:1280–1288. <https://doi.org/10.1021/acsami.5b09965>
43. Liu S, Liu W, Liu Y, Lin JH, Zhou X, Janik MJ, Colby RH, Zhang Q (2010) Influence of imidazolium-based ionic liquids on the performance of ionic polymer conductor network composite actuators. *Polym Int* 59:321–328. <https://doi.org/10.1002/pi.2771>
44. Lee JW, Hong SM, Koo CM (2014) High-performance polymer ionomer-ionic liquid membrane IPMC actuator. *Res Chem Intermed* 40:41–48. <https://doi.org/10.1007/s11164-013-1453-0>
45. Pandita SD, Lim HT, Yoo Y, Park HC (2006) Degradation mechanism of ionic polymer actuators containing ionic liquids as a mixed solvent. *Smart Struct Mater 2006 Electroact Polym Actuators Devices* 6168:616816. <https://doi.org/10.1117/12.658115>
46. Kim D, Kim KJ (2006) Electro-chemo-mechanical interpretation of Pt and Au-electroded relaxationless ionic polymer-metal composites. *Smart Struct Mater 2006 Electroact Polym Actuators Devices* 6168:616811. <https://doi.org/10.1117/12.654740>
47. Tang Y, Xue Z, Xie X, Zhou X (2016) Ionic polymer-metal composite actuator based on sulfonated poly(ether ether ketone) with different degrees of sulfonation, sensors actuators. *A Phys* 238:167–176. <https://doi.org/10.1016/j.sna.2015.12.015>
48. Altunkaya E, Seki Y, Çetin L, Gürses BO, Özdemir O, Sever K, Sarıkanat M (2018) Characterization and analysis of motion mechanism of electroactive chitosan-based actuator. *Carbohydr Polym* 181:404–411. <https://doi.org/10.1016/j.carbpol.2017.08.113>
49. Lee JW, Kim JH, Goo NS, Lee JY, Yoo YT (2010) Ion-conductive poly(vinyl alcohol)-based IPMCs. *J Bionic Eng* 7:19–28. [https://doi.org/10.1016/S1672-6529\(09\)60194-3](https://doi.org/10.1016/S1672-6529(09)60194-3)
50. Vunder V, Hamburg E, Johanson U, Punning A, Aabloo A (2016) Effect of ambient humidity on ionic electroactive polymer actuators. *Smart Mater Struct* <https://doi.org/10.1088/0964-1726/25/5/055038>
51. Wang HS, Cho J, Song DS, Jang JH, Jho JY, Park JH (2017) High-performance electroactive polymer actuators based on ultrathick ionic polymer-metal composites with nanodispersed metal electrodes. *ACS Appl Mater Interfaces* 9:21998–22005. <https://doi.org/10.1021/acsami.7b04779>
52. Liu S, Lin M, Zhang Q (2008) Extensional ionomeric polymer conductor composite actuators with ionic liquids. *Electroact Polym Actuators Devices* 2008 6927:69270H. <https://doi.org/10.1117/12.787597>
53. Safari M, Naji L, Baker RT, Taromi FA, Sun Z, Zhao G, Guo H, Xu Y (2015) The enhancement effect of lithium ions on actuation performance of ionic liquid-based IPMC soft actuators. *Polym (Guilfd)* 76:140–149. <https://doi.org/10.1016/j.polymer.2015.09.004>
54. Hong W, Almomani A, Montazami R (2014) Influence of ionic liquid concentration on the electromechanical performance of ionic electroactive polymer actuators. *Org Electron Physics Mater Appl* <https://doi.org/10.1016/j.orgel.2014.08.036>
55. He Q, Vokoun D, Stalbaum T, Kim KJ, Fedorchenko AI, Zhou X, Yu M, Dai Z (2019) Mechanoelectric transduction of ionic polymer-graphene composite sensor with ionic liquid as electrolyte. *Sens Actuators Phys* 286:68–77. <https://doi.org/10.1016/j.sna.2018.12.014>
56. Bian C, Zhu Z, Bai W, Chen H, Li Y (2020) Fast actuation properties of several typical IL-based ionic electro-active polymers under high impulse voltage. *Smart Mater Struct* <https://doi.org/10.1088/1361-665X/ab6882>
57. Da Trindade LG, Zanchet L, Padilha JC, Celso F, Mikhailenko SD, Becker MR, De Souza MO, De Souza RF (2014) Influence of ionic liquids on the properties of sulfonated polymer membranes. *Mater Chem Phys* 148:648–654. <https://doi.org/10.1016/j.matchemphys.2014.08.030>
58. Fulmer GR, Miller AJM, Sherden NH, Gottlieb HE, Nudelman A, Stoltz BM, Bercaw JE, Goldberg KI (2010) NMR chemical shifts of trace impurities: common laboratory solvents, organics, and gases in deuterated solvents relevant to the organometallic chemist. *Organometallics* 29:2176–2179. <https://doi.org/10.1021/om100106e>
59. Lian C, Liu K, Van Aken KL, Gogotsi Y, Wesolowski DJ, Liu HL, Jiang DE, Wu JZ (2016) Enhancing the capacitive performance of electric double-layer capacitors with ionic liquid mixtures. *ACS Energy Lett* 1:21–26. <https://doi.org/10.1021/acseenergylett.6b00010>
60. Drozdov AD (2016) Modeling the response of polymer-ionic liquid electromechanical actuators. *Acta Mech* 227:437–465. <https://doi.org/10.1007/s00707-015-1471-7>

Publisher's Note Springer Nature remains neutral with regard to jurisdictional claims in published maps and institutional affiliations.

Springer Nature or its licensor (e.g. a society or other partner) holds exclusive rights to this article under a publishing agreement with the author(s) or other rightsholder(s); author self-archiving of the accepted manuscript version of this article is solely governed by the terms of such publishing agreement and applicable law.